Nanotransfer-on-things: From rigid to stretchable nanophotonic devices

Junseong Ahn[a,b], Jimin Gu[a], Yongrok Jeong[a,b], Ji-Hwan Ha[a,b], Jiwoo Ko[a], Byeongmin Kang[a,b], Soon Hyoung Hwang[b], Jaeho Park[a], Sohee Jeon[b], Hwi Kim[c], Jun-Ho Jeong[b], Inkyu Park[a*]*

[a]Department of Mechanical Engineering, Korea Advanced Institute of Science and Technology (KAIST), Daejeon 34141, Republic of Korea

[b]Department of Nano Manufacturing Technology, Korea Institute of Machinery and Materials (KIMM), Daejeon 34103, Republic of Korea

[c]Department of Electronics and Information Engineering, Korea University, Sejong 30019, Republic of Korea

KEYWORDS. nanotransfer printing, nanophotonic devices, hologram, color filter, optical strain sensor.

ABSTRACT. The growing demand for nanophotonic devices has driven the advancement of nanotransfer printing (nTP) technology. Currently, the scope of nTP is limited to certain materials and substrates owing to the temperature, pressure, and chemical bonding requirements. In this study, we developed a universal nTP technique utilizing covalent bonding-based

adhesives to improve the adhesion between the target material and substrate. Additionally, the technique employed plasma-based selective etching to weaken the adhesion between the mold and target material, thereby enabling the reliable modulation of the relative adhesion forces, regardless of the material or substrate. The technique was evaluated by printing four optical materials on nine substrates, including rigid, flexible, and stretchable substrates. Finally, its applicability was demonstrated by fabricating a ring hologram, a flexible plasmonic color filter, and extraordinary optical transmission-based strain sensors. The high accuracy and reliability of the proposed nTP method were verified by the performance of nanophotonic devices that closely matched numerical simulation results.

Introduction

Research pertaining to precisely designed nanophotonic devices on various substrates has recently received considerable attention driven by the growing demand for diverse mechanical and optical properties in optical elements, such as those used in augmented reality (AR) and virtual reality (VR) systems[1], sensors[2], lenses[3], and flexible and stretchable displays[4]. In this regard, nanotransfer printing (nTP) has been extensively studied in industry and academia as a fabrication technique because of its ability to repeatedly produce large-area nanostructures with high efficiency[5–8]. The basic mechanism of nTP relies on the adhesion force between the mold and material (F_1) being weaker than the adhesion force between the material and substrate (F_2)[9]. The relative adhesion force is defined as F_2 - F_1, and material transfer to the substrate is possible under the condition: $F_2 - F_1 > 0$. Currently, nTP methods focus on either reducing F_1 or increasing F_2 to generate a high relative adhesion force. However, these methods remain limited

in terms of the range of compatible materials and substrates, as well as process reliability. Particularly, thermomechanically-assisted nTP, which relies on generating a stronger F_2 through mechanical interlocking, has gained recognition for its simplicity and diversity of compatible materials[10]. However, it is exclusively applicable to limited thermoplastic polymer substrates. In contrast, sacrificial layer-assisted nTP, which relies on reducing the F_1 to approximately zero through removal of the mold, is a more commonly used strategy owing to its wide-range compatibility. However, the surface tension of the liquid etchants can lead to detrimental effects on the fabrication yield because the F_2, based purely on van der Waals forces, is weak[11]. Additionally, when the substrate is unable to absorb the liquid etchant containing the dissolved sacrificial polymer, the polymer residue may remain on the transferred material[12]. Chemical-assisted nTP is also a viable option, which involves the use of a self-assembled monolayer (SAM) as an adhesive between the target material and substrate to increase the F_2. However, some SAM adhesives are only compatible with certain materials (e.g., thiol–Au interaction[13]). The more universal chemical adhesives (e.g., the interaction between silicon atoms of the adhesive layer and oxygen atoms of deposited materials[14]) have a relatively weak F_2 compared with that of thermomechanically-assisted nTP. This complicates the use of SAM in nTP when the F_1 is high[14]. In addition, the adhesion force generated via the aforementioned methods depends on the target transfer material, the equipment used, and the condition of the adhesive. For example, for the thiol–Au interaction, the adhesion force cannot be controlled. Therefore, monolithic transfer methods, which do not offer control over the relative adhesion forces, are difficult to use for general transfer processes. These limitations require users to adopt different transfer methods depending on the specific materials, substrates, and equipment used in each application. Furthermore, they prevent the direct use of highly sought-after stretchable substrates for

nanophotonic devices owing to the complex nanotransfer conditions that are required. Therefore, developing an nTP method with a wide range of material and substrate compatibility and a reliable process remains a significant challenge.

To overcome these limitations, this study presents the development of a universal and reliable nTP technique that can be used with a wide range of optical materials and substrates. The technique employs covalent bonding-based adhesives to strengthen the F_2, whereas plasma-based selective etching weakens the F_1. The adhesion force, F_1, can be modulated by adjusting the plasma etching time. The developed nTP method can be conducted without plasma etching for combinations of materials and substrates that exhibit a high relative adhesion force. Additionally, this method can be applied with plasma etching for combinations of materials and substrates that have an intrinsically low relative adhesion force. The universality of the developed nTP method was demonstrated through the successful printing of four optical materials on nine different substrates, including rigid, flexible, and stretchable substrates. Finally, its applicability was demonstrated through the creation of a ring hologram with Al on an Al_2O_3 wafer, a flexible plasmonic color filter (PCF) with Ag on a polyethylene terephthalate (PET) substrate, and an extraordinary optical transmission (EOT)-based strain sensor with TiO_2 on a polydimethylsiloxane (PDMS) substrate. This study helps expand the limited literature available on universal nTP techniques for nanophotonic devices, which represents the contribution of the technique developed in this study, as summarized in Table S1. Furthermore, we have pioneered the rational design and implementation of an EOT-based soft strain sensor using a stretchable substrate.

Overall nTP concept

Figure 1 shows the overall concept of the developed nTP technique and its application to nanophotonic devices. In this study, we demonstrated nTP of four optical materials (i.e., Ag, Au/SiO_2/Au, Al, and TiO_2) on nine different substrates (i.e., three rigid substrates: Si, SiO_2, and Al_2O_3 wafers; three flexible substrates: poly(methyl methacrylate) (PMMA), PET, colorless polyimide (CPI); and stretchable substrates: PDMS, Dragon SkinTM, thermoplastic polyurethane (TPU)), as shown in Figure 1a. This demonstrates the material and substrate diversity of the developed nTP method, addressing a limitation of the conventional nTP techniques. Two mechanisms are selectively used to realize transfer printing with versatile substrates and diverse materials depending on the intrinsic relative adhesion force. As depicted in Figure 1b-i, for materials with low intrinsic adhesion with a poly(urethane acrylate) (PUA) mold (i.e., Ag and Au/SiO_2/Au in this study), the developed method utilizes covalent bonding-assisted conventional nTP, which we previously developed[14,15]. This is because forming covalent bonding between substrates and materials is sufficient to induce a high relative adhesion force. In this process, an ultrathin (sub-10-nm) layer of an organic ligand, N-[3-(trimethoxysilyl)propyl]ethylenediamine, is used to promote adhesion and enable strong covalent bonding. However, for materials with high intrinsic adhesion to the PUA mold (i.e., Al and TiO_2 in this study), the plasma etching process is additionally used before applying covalent bonding-assisted nTP, as shown in Figure 1b-ii.

O_2 plasma treatment activates the hydroxyl groups on the surface of the target material to facilitate stronger covalent bonding with the substrates and selectively etches the nanopatterned PUA mold. The etching of the PUA mold reduces the area of the mold contacting the target material, thereby weakening the adhesion. Therefore, the relative adhesion force can be controlled by varying the amount of plasma etching. This demonstrates that the developed nTP

technique has the potential to be applied to arbitrary materials and substrates in different environments by appropriately designing plasma etching depending on the selected material and substrate.

Various nanophotonic devices were fabricated to demonstrate the applicability of the developed nTP, as shown in Figure 1c. As examples of essential optical elements in display technologies, we designed and fabricated a reflection ring hologram with TiO_2 on an Al_2O_3 wafer and a flexible PCF with Ag on a PET substrate with trichromatic colors of red, green, and blue. In addition, an EOT-based soft strain sensor with TiO_2 on a PDMS substrate was proposed. In the strain sensor, the distance between the circular pattern array was altered under applied strain, resulting in a change in the transmittance peak. The applied strain can be calculated by measuring the change in the transmittance peak of the sensor, as explained in detail in the following sections.

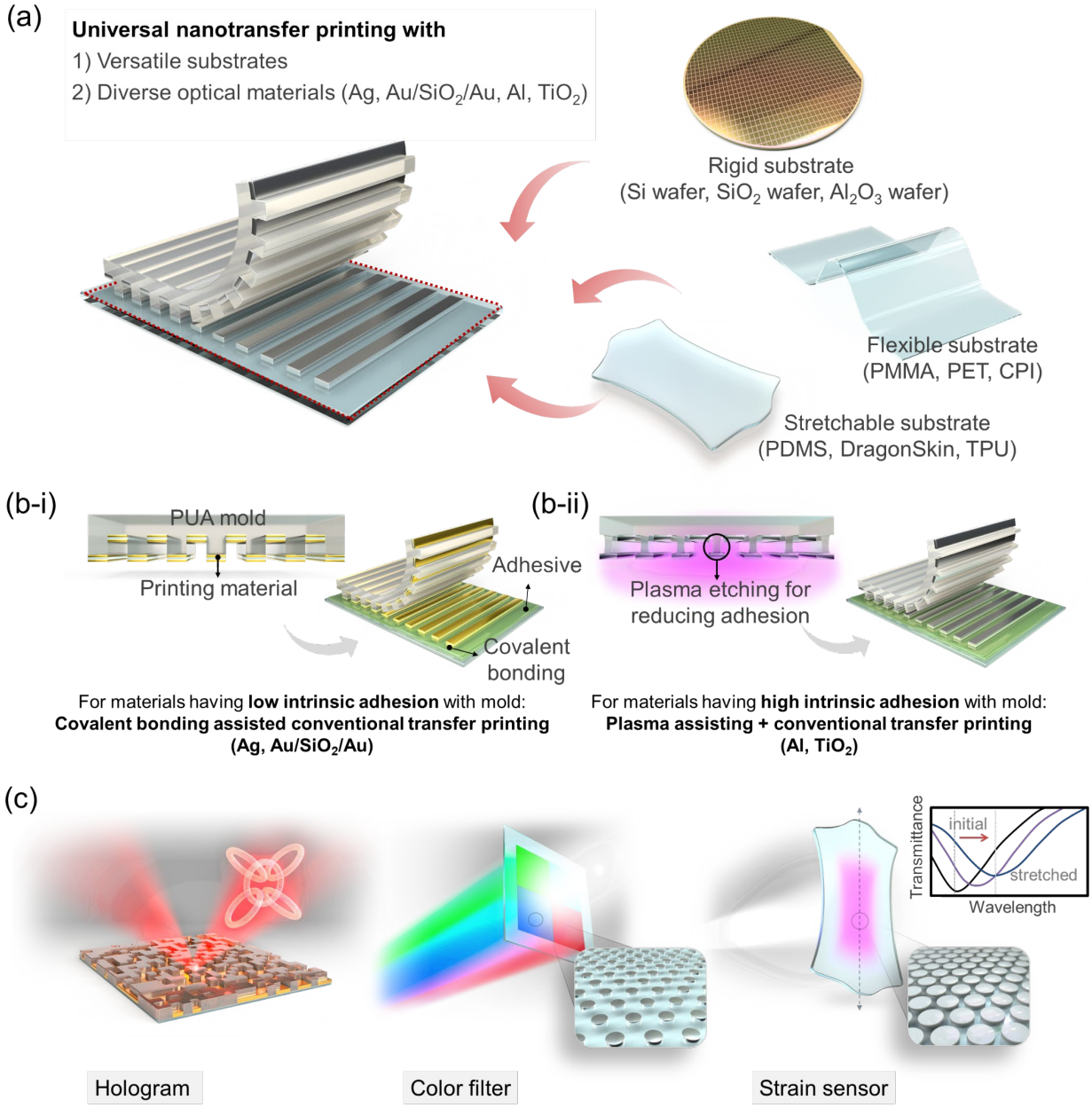

Figure 1: Concept of universal nTP and its applications to nanophotonic devices **a.** Overall scheme of universal nTP with various target materials and substrates. **b.** Mechanism of b-i, covalent bonding-assisted conventional transfer printing, and b-ii, additional plasma-assisted

transfer printing. **c.** Nanophotonic devices fabricated by the developed nTP: reflection ring hologram, flexible PCF, and EOT-based soft strain sensor.

Results of nTP with diverse optical materials on diverse substrates

Figure 2 shows the effects of the plasma etching process on the nTP and the results of the developed nTP technique. As shown in Figures 2a and S1, materials exhibiting a high intrinsic adhesion force with the PUA mold (i.e., materials with a low relative adhesion force, TiO_2 in this study) are not transferred using only the conventional adhesive based on covalent bonding. A detailed explanation of the covalent bonding-assisted nTP is described in our previous study[14,15]. O_2 plasma selective etching was applied to reduce the contact area between the PUA mold and TiO_2, thereby reducing the adhesion force between them. When the diameter of the circular pattern of the PUA is reduced from 230 nm to 65 nm by plasma etching, TiO_2 is successfully transferred onto the PDMS substrate. Notably, when the PUA mold is over-etched, the unwanted region that deposited TiO_2 on the trench of the nanopattern is also transferred, indicating the possibility of an optimal condition depending on the materials and substrates, as shown in Figures S2 and S3. By adjusting the plasma conditions, four optical materials can be transferred onto nine different substrates, as shown in Figure 2b. Additional experiments showing applicability with other materials are described in Figure S4. Using the proposed method, most of the materials compatible with the e-beam evaporation process can be fabricated on the donor mold and transferred onto the target substrate regardlesss of their intrinsic adhesion force. Also, the surface roughness of the target material did not change even after O_2 plasma treatment, as shown in Figure S5, and the transferred materials maintain their original shapes and material properties after the nTP process, as shown in Figure 2c. In addition, polymer residue is not

observed on the transferred material, as shown in Figure S6. In these experiments, various nanopatterns with small sizes of up to 50 nm (shown in Figure S7), including lines and crosses, circles, and random rectangular patterns, were used to demonstrate the diversity of shape and size of the mold. Although the intrinsic relative adhesion force can be affected by various factors such as materials, substrates, molds, and the fabrication environment, the optimal plasma condition, which is adjustable, is determined solely by the width of the nanopattern and the types of materials used in this study. These parameters are sufficient for transferring the abovementioned materials on the target substrates. The detailed experimental conditions are described in Table S2.

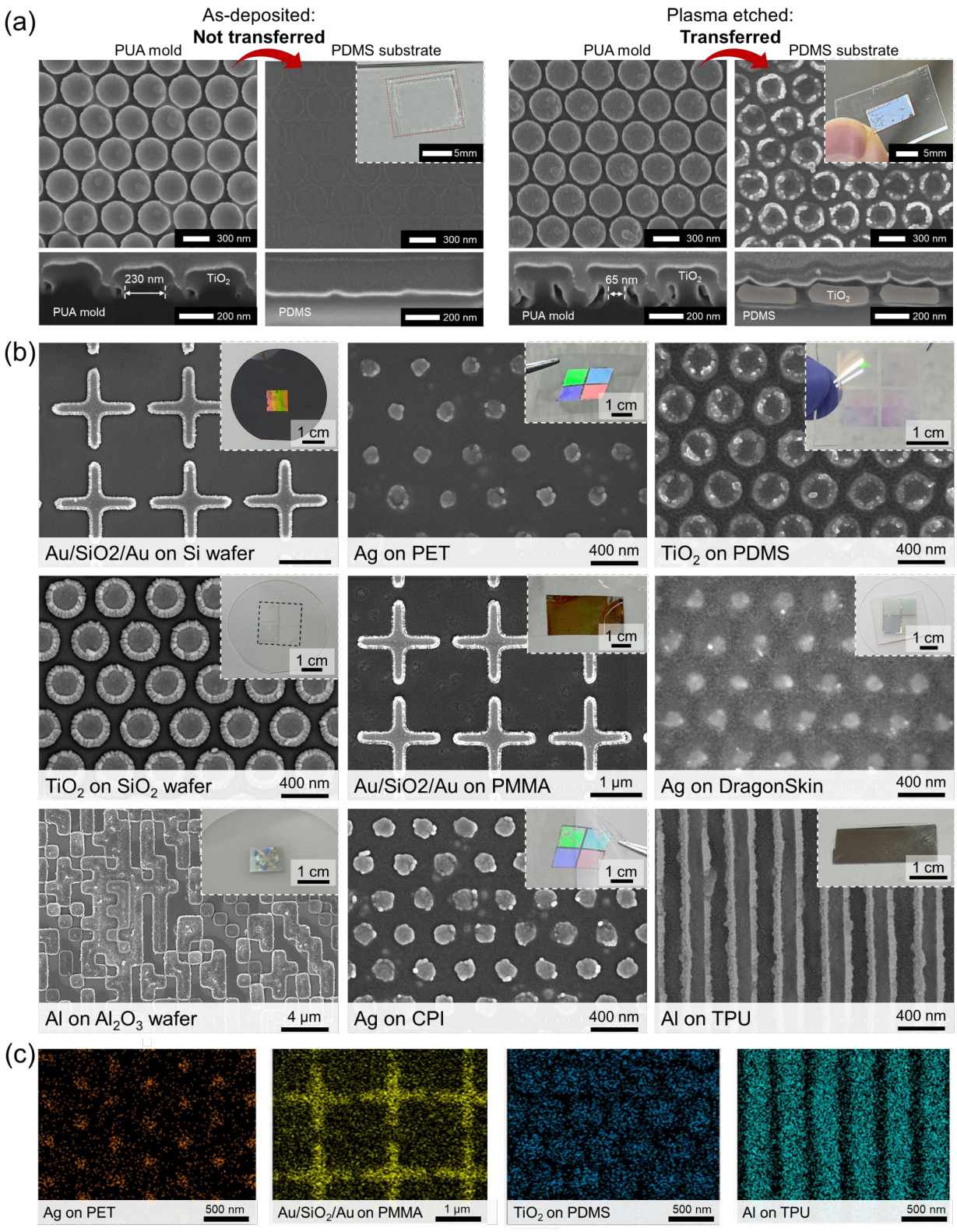
(a)
As-deposited:
Not transferred
PUA mold
PDMS substrate
Plasma etched:
Transferred
PUA mold
PDMS substrate
300 nm
5mm
230 nm
TiO2
PUA mold
200 nm
PDMS
65 nm
(b)
1 cm
Au/SiO2/Au on Si wafer
Ag on PET
400 nm
TiO2 on PDMS
TiO2 on SiO2 wafer
Au/SiO2/Au on PMMA
1 μm
Ag on DragonSkin
Al on Al2O3 wafer
4 μm
Ag on CPI
Al on TPU
(c)
Ag on PET
500 nm
Au/SiO2/Au on PMMA
TiO2 on PDMS
Al on TPU

Figure 2: Results of nTP with diverse optical materials on diverse substrates **a.** Top- and side-view scanning electron microscopy (SEM) images depicting the nTP results of TiO_2 from PUA mold to PDMS substrate with and without plasma assistance. **b.** Top-view SEM images and photographs showing the results of nTP with four optical materials on nine different substrates. This experiment used various nanopatterns, including line and crosses, circles, and random rectangular patterns. **c.** EDS mapping images of four optical materials transferred on various substrates.

Applications as nanophotonic devices fabricated by the developed nTP technique: hologram and flexible PCF

To demonstrate the broad applicability of nTP, two representative nanophotonic devices were fabricated and characterized: (1) a hologram and (2) a flexible PCF. Figure 3a shows the fabricated reflection Al-ring hologram on a rigid Al_2O_3 wafer substrate. First, to achieve a ring hologram using the developed nTP technique, a Si master mold is fabricated with nanopatterns designed using a polygon-based computer-generated hologram (CGH) synthesis algorithm, as shown in Figure S8a[16]. Subsequently, Al, which shows excellent plasmonic characteristics[15], is deposited on the PUA mold replicated from the Si master using a UV-curable resin. It is successfully transferred on a cm-scale on the Al_2O_3 wafer, as shown in Figures 3a and 3b. When incident light with different trichromatic colors (i.e., red, green, and blue) is applied, a hologram composed of five rings with the corresponding colors is generated, as shown in Figure 3c. The experimental setup is shown in Figure S4. By integrating three light sources, every color can be realized. In addition, in the design process, the hologram is designed to rotate depending on the angle of the incident light. A rotating hologram under different angles of incident light

demonstrates the possibility of realizing arbitrary nanopatterns on target substrates with a large area and high accuracy using the developed nTP, as shown in Figure 3d and Video S1.

Second, a Si master is designed to demonstrate the flexible PCF using a finite-difference time-domain (FDTD) simulation, as shown in Figure S8b. The Ag circular pattern array is thereafter transferred onto the PET substrate using the same process as that used for fabricating the hologram, as shown in Figure 3e. The working principle of the PCF is based on the EOT phenomenon, and the color depends on the pattern size and pitch of the pattern. Therefore, four nanopatterns are designed and fabricated to realize the trichromatic colors of light as well as purple, as shown in Figure 3f. The fabricated flexible PCF on the PET substrate reveals sharp optical transmittance peaks (corresponding to red, green, blue, and purple) at the corresponding wavelengths, which are in good agreement with the simulation results obtained in the design process, as shown in Figure 3g. The detailed design and simulation parameters are shown in Figure S10 and Table S3.

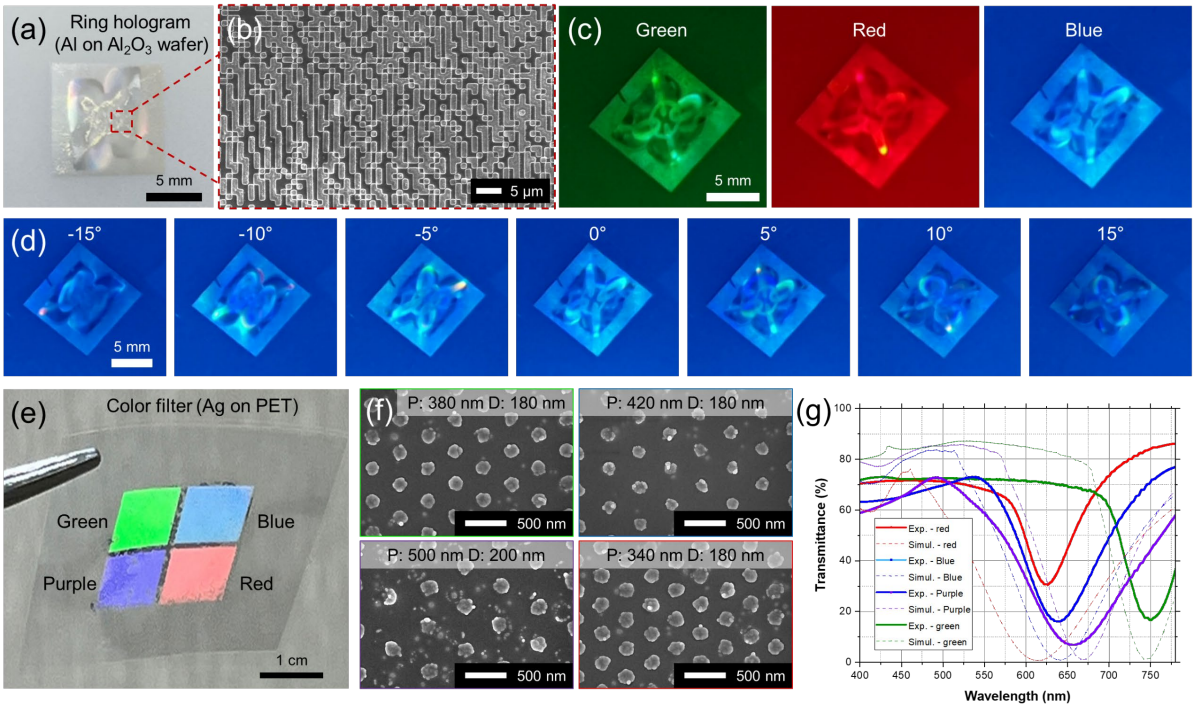

Figure 3: Nanophotonic devices fabricated through the developed nTP technique: hologram and flexible PCF **a.** Photographic and **b.** top-view SEM images of the fabricated reflection Al-ring hologram on an Al_2O_3 wafer substrate. **c.** Ring holograms with different colored light sources: green, red, and blue. **d.** Blue ring holograms under the light source with different incident angles ranging from −15° to 15° with an interval of 5°. **e.** Photograph and **f.** top-view SEM images of the fabricated flexible Ag PCF on a PET substrate. The four PCF regions represent different colors, including the trichromatic light colors. **g.** Experimental and FDTD simulation results of the fabricated and designed flexible PCF.

Application as nanophotonic device fabricated by the developed nTP technique: strain sensor

We demonstrated an EOT-based soft strain sensor to validate that the developed universal nTP technique can be used to create nanophotonic devices beyond display technology. The growing demand for soft strain sensors in various fields, such as structural health and human motion monitoring[17], has led to the development of a wide range of strain sensors, including resistive-[18], capacitive-[19], and optical-[20] type strain sensors. Among them, optical-type strain sensors, based on the optical transmittance change in a functional film under an applied strain, have attracted considerable attention because of their fast and linear response and low hysteresis[21]. However, existing sensors have a critical disadvantage. A reference detector and additional calibration are required because the sensing signal varies depending on the change in the external light intensity, rendering the systems bulky and complicated[17]. We propose an EOT-based soft strain sensor to overcome this limitation. The effect of external light intensity can be eliminated by measuring the change in the peak wavelength of the transmittance graph caused by the EOT phenomenon. The EOT-based TiO_2 strain sensor is designed to exhibit a sharp transmittance peak, maintaining the original peak wavelength in response to the change in external light. The corresponding Si master mold is fabricated as shown in Figure S3c.

In this study, PDMS substrate was used because of its stretchability and high optical transmittance, and TiO_2 was chosen because of its low optical loss, high refractive index (n), and low extinction coefficient (k), enabling the realization of a sharp transmittance peak[22]. When strain is applied to the strain sensor composed of a TiO_2 circular pattern array on PDMS, the distance between each pattern increases. Therefore, the corresponding peak wavelength changes owing to the EOT phenomenon. Notably, because of the difference in Young's modulus between TiO_2 and PDMS, most of the applied surface strain is concentrated in the PDMS region (i.e., the region between the TiO_2 patterns)[12]. This not only allows for the maximum optical peak change

resulting from the change in the gap between the TiO_2 patterns but also enables the TiO_2 patterns to maintain their original shape without cracking during the stretching and releasing of the sensor. Figure 4a shows the EOT-based TiO_2 strain sensor loaded on the linear stage with the PDMS substrate. Whereas the overall transmittance changes when measuring the optical transmittance of the sensor at wavelengths ranging from 500 to 600 nm under different light intensities (i.e., 26.51, 17.22, and 9.78 W/m^2), the shape and tendency of the peak change under different applied strains are similar, as shown in Figure 4b. The peak wavelength gradually increases as the applied strain increases from 0 to 12.5% at intervals of 1.25%, as shown in Figure 4c. The tendency of the peak change depending on the applied strain in the experiment with different light intensities is in good agreement with the FDTD simulation results, as shown in Figures 4d and S11. The detailed simulation conditions are described in Table S4. Particularly, the strain sensor exhibits a highly linear response with an R_2 value of 0.997 and a sensitivity of 1.96 nm/% under a light intensity of 26.51 W/m^2. The peak wavelengths for the experimental results under the light intensity of 17.22 and 9.78 W/m^2 are only recorded until 10% and 7.5% strain, respectively, as shown in Figure 4d. This result is attributed to the difficulty encountered in accurately measuring the peak wavelength under low-power light using our spectrometer. However, the overall shape of the transmittance graph remains unchanged compared with that under high-power light, as shown in Figure S12. Subsequently, a cyclic test was conducted to verify the mechanical robustness of the developed strain sensor. The applied strain is mostly concentrated on the exposed PDMS region. The TiO_2 pattern maintains its original shape and peak wavelength even after repeated 1,000 cyclic tests with an external strain of 10%, as shown in Figures 4e and 4f.

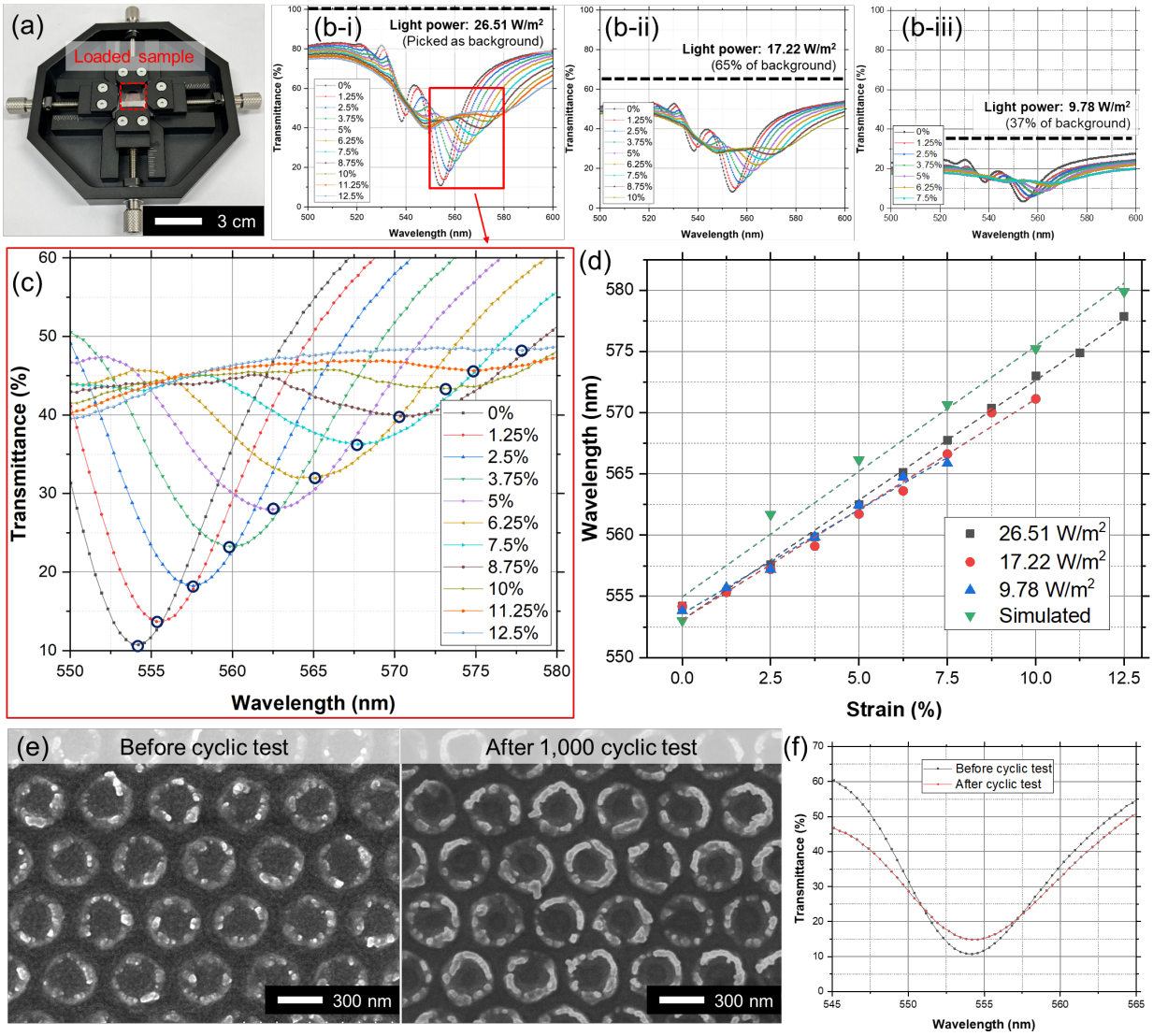

Figure 4: Nanophotonic device fabricated by the developed nTP technique: strain sensor **a.** Photograph of the EOT-based TiO_2 strain sensor with the PDMS substrate loaded on a linear stage. **b.** Transmittance graph of the strain sensor under the light power of b-i. 26.51, b-ii. 17.22, and b-iii. 9.78 W/m^2 depending on the applied external strain, showing the effects of light intensity on the sensing performance. **c.** Enlarged transmittance graph depending on the applied external strain under the light power of 26.5 W/m^2. **d.** Experimental and FDTD simulation results show the transmittance peak wavelength depending on the light intensity and applied

external strain. **e.** Top-view SEM images of the strain sensor, and **f.** enlarged transmittance graph before and after the repeated 1,000 cyclic tests with an external strain of 10%.

Conclusion

We proposed a universal and reliable nTP method that could be used with a variety of optical materials and substrates. In addition to the conventional covalent bonding-based nTP, plasma etching of the PUA mold facilitated the modulation of the relative adhesion force, enabling nTP regardless of the materials and substrates. To demonstrate the universality of our method, we printed four optical materials (i.e., Ag, Au/SiO_2/Au, Al, and TiO_2) on nine different substrates (i.e., three rigid substrates: Si wafer, SiO_2 wafer, and Al2O3 wafer; three flexible substrates: PMMA, PET, and CPI; and stretchable substrates: PDMS, Dragon SkinTM, and TPU). Finally, the applicability was verified by designing and demonstrating a ring hologram with TiO_2 on an Al_2O_3 wafer, a flexible PCF with Ag on a PET substrate, and an EOT-based strain sensor with TiO_2 on a PDMS substrate. In all applications, the performance of the fabricated nanophotonic devices matched well with the FDTD simulation results, showing the high accuracy and reliability of the developed nTP method even in large-area device fabrication. Overall, we could realize large-area devices of up to a few centimeters for commercialization, whereas the devices fabricated via e-beam lithography are on a scale of a few millimeters[23]. In addition, the high material diversity enabled nTP on elastomeric substrate, thereby yielding the first demonstration of an EOT-based soft strain sensor designed by FDTD simulation.

However, certain challenges need to be addressed to advance nTP. In the case of various nanopatterns of different sizes and shapes on a single mold, the optimal plasma conditions can vary depending on the individual patterns, even on the same mold. Because the O_2 plasma treatment simultaneously etches all the nanopatterns, the materials deposited on a single mold

composed of various nanopatterns with different sizes and shapes (e.g., a combination of micropatterns and nanopatterns) may not be uniformly transferred. The hologram nanopattern, composed of various rectangular shapes with different sizes, was successfully transferred onto the substrates after plasma etching. We expect that a range of transferrable conditions (i.e., the transferrable range for the amount of plasma etching) exists depending on the sizes and shapes of the nanopatterns. Therefore, nTP will be possible within the overlapping range between the transferrable conditions of each pattern, even if the pattern size is different. Subsequent research should analyze and confirm the aforementioned hypothesis to further develop a universal nTP method.

Despite this limitation, we believe that the proposed nTP technique could help resolve the bottleneck related to material and substrate diversity[24], as well as the reliability of previous nTP methods. Moreover, it will pave the way to extend the applicability of nTP and facilitate commercialization through the fabrication of nanophotonic devices, such as flexible and stretchable AR and VR systems, sensors, lenses, and displays.

Methods

Fabrication of the nanopatterned PUA mold: A Si master mold was prepared using krypton fluoride lithography. RM-311 polyurethane resin (Minuta Technology Co., Ltd., Korea) was poured into the prepared Si master and covered with a UV-transparent PET film for polymer mold replication. Proper pressure was applied to the resin using a hand roller to facilitate the complete penetration of the resin into the nanopatterns of the master mold. Subsequently, the resin was cured under UV light and separated from the master mold. The detailed fabrication of the polymer mold from the Si master has been described in our previous work[25,26].

Procedure of the developed nTP method with and without plasma assistance: Target optical materials (Ag, Au/SiO_2/Au, Al, and TiO_2) were deposited on the nanopatterned PUA mold using an e-beam evaporator (Daeki Hi-Tech Co., Ltd., Korea). Thereafter, O_2 plasma treatment under the optimal conditions (Table S2) was applied to the PUA mold with the target material. The plasma power was set at 100 W, and the treatment was used to selectively etch and activate the target material surface on the PUA mold. The adhesion promoter, N-[3-(trimethoxysilyl)propyl]ethylenediamine, was spin-coated onto the target substrate at 5000 rpm for 1 min. The substrate was heated on a hot plate at 150 ℃ for 1 min to evaporate the solvent and activate the dangling bonds of the adhesion promoter. The plasma-assisted PUA mold with the target material was placed on the target substrate and pressed using a hand roller on a hot plate to facilitate conformal contact. After 4 min at 150 ℃, the mold was detached from the substrate, and the target material was transferred onto the target substrate.

Surface characterization of the transferred nanopatterns: The surface characteristics were evaluated using field-emission SEM combined with energy-dispersive X-ray spectroscopy (EDS) (Sirion, FEI, the Netherlands) and focused ion-beam SEM (Helios Nanolab, FEI, the Netherlands).

Fabrication and characterization of the hologram, color filter, and strain sensor: An Al-ring hologram on an Al_2O_3 wafer substrate was designed using a polygon-based CGH synthesis algorithm, as described in our previous work[16]. To graphically measure the rotating ring holograms with three different colors (red, green, and blue), a customized optical setup and commercial flashlights were used, as shown in Figure S9. Flexible Ag PCF and EOT-based TiO_2 strain sensors were designed using FDTD simulation (FDTD Solutions, Lumerical Inc., Canada). In both applications, the wavelength dependence of optical transmittance was measured using

optical spectroscopy. In addition, a customized linear stage was used to apply 1-axis strain to the strain sensor. To eliminate the influence of Poisson's effect, the end sites in the direction perpendicular to the applied strain were fixed during the experiments, which prevented deformation in that direction. All three nanophotonic devices were fabricated using the aforementioned nTP process.

ASSOCIATED CONTENT

AUTHOR INFORMATION

Corresponding Author

*Corresponding Author. E-mail: inkyu@kaist.ac.kr (I. Park); jhjeong@kimm.re.kr (J.-H. Jeong)

ACKNOWLEDGMENT

J. Ahn, J. Gu, and Y. Jeong contributed equally to this study. This work was supported by a National Research Foundation of Korea (NRF) grant funded by the Korean government (MSIT) (No. 2021R1A2C3008742), Institute of Information & Communications Technology Planning & Evaluation (IITP) grant funded by the Korea government (MSIT) (No. 2020-0-00914, Development of hologram printing downsizing technology based on holographic optical element(HOE)), and the Development Program of Machinery and Equipment Industrial Technology (20018235, Development of inline nano-imprinter for nanophotonic device) funded by the Ministry of Trade, Industry & Energy(MI, Korea).

REFERENCES

1. Park, J. Y.; Cho, W. S.; Choi, C. S.; Cho, S. H.; Lee, J. L. Embedding scattering centers in polymer substrate to yield robust hazy film with high optical transmittance: application to virtual-reality display. *Adv. Opt. Mater.* **2020**, 8, 1901866. DOI: 10.1002/adom.201901866

2. Shi, X.; Verschueren, D. V.; Dekker, C. Active delivery of single DNA molecules into a plasmonic nanopore for label-free optical sensing. *Nano Lett.* **2018**, 18, 8003–8010. DOI: 10.1021/acs.nanolett.8b04146

3. Ko, J.; Kang, H.; Ahn, J.; Zhao, Z.; Jeong, Y.; Hwang, S. H.; Bok, M.; Jeon, S.; Gu, J.; Ha, J.; Rho, J.; Jeong, J.; Park, I. Biocompatible nanotransfer printing based on water bridge formation in hyaluronic acid and its application to smart contact lenses. *ACS Appl. Mater. Interfaces* **2021**, 13, 35069–35078. DOI: 10.1021/acsami.1c06225

4. Xiong, K.; Tordera, D.; Jonsson, M. P.; Dahlin, A. B. Active control of plasmonic colors: Emerging display technologies. *Rep. Prog. Phys.* **2019**, 82. DOI 10.1088/1361-6633/aaf844

5. Zhao, Z. J.; Ahn, J.; Hwang, S. H.; Ko, J.; Jeong, Y.; Bok, M.; Kang, H. J.; Choi, J.; Jeon, S.; Park, I.; Jeong, J. H. Large-area nanogap-controlled 3D nanoarchitectures fabricated via layer-by-layer nanoimprint. *ACS Nano* **2021**, 15, 503–514. DOI: 10.1021/acsnano.0c05290

6. Han, Y.; Han, H. J.; Rah, Y.; Kim, C.; Kim, M.; Lim, H.; Ahn, K. H.; Jang, H.; Yu, K.; Kim, T. S.; Cho, E. N.; Jung, Y. S. Desolvation-triggered versatile transfer-printing of pure BN films with thermal-optical dual functionality. *Adv. Mater.* **2020**, 32, 2002099. DOI:10.1002/adma.202002099

7. Nam, T. W.; Kim, M.; Wang, Y.; Kim, G. Y.; Choi, W.; Lim, H.; Song, K. M.; Choi, M. J.; Jeon, D. Y.; Grossman, J. C.; Jung, Y. S. Thermodynamic-driven polychromatic quantum dot patterning for light-emitting diodes beyond eye-limiting resolution. *Nat. Commun.* **2020**, 11. DOI: 10.1038/s41467-020-16865-7

8. Kim, S.; Jiang, Y.; Thompson Towell, K. L.; Boutilier, M. S. H.; Nayakanti, N.; Cao, C.; Chen, C.; Jacob, C.; Zhao, H.; Turner, K. T.; Hart, A. J. Soft nanocomposite electroadhesives for digital micro-and nanotransfer printing. *Sci. Adv.* **2019**, 5. DOI: 10.1126/sciadv.aax4790

9. Hur, S. H.; Khang, D. Y.; Kocabas, C.; Rogers, J. A. Nanotransfer printing by use of noncovalent surface forces: Applications to thin-film transistors that use single-walled carbon nanotube networks and semiconducting polymers. *Applied Physics Letters*, **2004**, 85, 5730–5732. DOI: 10.1063/1.1829774

10. Jeong, Y.; Kang, H.; Zhao, Z.; Ahn, J.; Hwang, S. H.; Jeon, S.; Ko, J.; Jung, J.; Park, I.; Jeong, J. Robust nanotransfer printing by imidization-induced interlocking. *Appl. Surf. Sci*. **2021**, 552, 149500. DOI: 10.1016/j.apsusc.2021.149500

11. Ko, J.; Zhao, Z. J.; Hwang, S. H.; Kang, H. J.; Ahn, J.; Jeon, S.; Bok, M.; Jeong, Y.; Kang, K.; Cho, I.; Jeong, J. H.; Park, I. Nanotransfer printing on textile substrate with water-soluble polymer nanotemplate. *ACS Nano* **2020**, 14, 2191-2201. DOI: 10.1021/acsnano.9b09082

12. Ahn, J.; Zhao, Z.; Choi, J.; Jeong, Y.; Hwang, S. H.; Ko, J.; Gu, J.; Jeon, S.; Park, J.; Kang, M.; Del Orbe, D.; Cho, I.; Kang, H.; Bok, M.; Jeong, J.; Park, I. Morphology-controllable wrinkled hierarchical structure and its application to superhydrophobic triboelectric nanogenerator. *Nano Energy* **2021**, 85. DOI: 10.1016/j.nanoen.2021.105978

13. Law, J. B. K.; Khoo, R. T. T.; Tan, B. S.; Low, H. Y. Selective gold nano-patterning on flexible polymer substrate via concurrent nanoimprinting and nanotransfer printing. *Appl. Surf. Sci.* **2011**, 258, 748–754. DOI: 10.1016/j.apsusc.2011.08.065

14. Hwang, S. H.; Jeon, S.; Kim, M.; Choi, D.; Choi, J. H.; Jung, J.; Kim, K.; Lee, J.; Jeong, J.; Youn, J. R. Covalent bonding-assisted nanotransfer lithography for the fabrication of plasmonic nano-optical elements. *Nanoscale* **2017**, 9, 14335–14346. DOI: 10.1039/C7NR02666H

15. Hwang, S. H.; Zhao, Z.; Jeon, S.; Kang, H.; Ahn, J.; Jeong J. H. Repeatable and metal-independent nanotransfer printing based on metal oxidation for plasmonic color filters. *Nanoscale* **2019**, 11, 11128–11137. DOI: 10.1039/C9NR00176J

16. Zhao, Z. J.; Hwang, S. H.; Kang, H. J.; Jeon, S.; Bok, M.; Ahn, S.; Im, D.; Hahn, J.; Kim, H.; Jeong, J. H. Adhesive-layer-free and double-faced nanotransfer lithography for a flexible large-area metasurface hologram. *ACS Appl. Mater. Interfaces* **2020**, 12, 1737–1745. DOI: 10.1021/acsami.9b14345

17. Gu, J.; Ahn, J.; Jung, J.; Cho, S.; Choi, J.; Jeong, Y.; Park, J.; Hwang, S. H.; Cho, I.; Ko, J.; Ha, J.; Zhao, Z.; Jeon, S.; Ryu, S.; Jeong, J.; Park, I. Self-powered strain sensor based on the piezo-transmittance of a mechanical metamaterial. *Nano Energy* **2021**, 89, 106447. DOI: 10.1016/j.nanoen.2021.106447

18. Kim, K. H.; Jang, N. S.; Ha, S. H.; Cho, J. H.; Kim, J. M. Highly sensitive and stretchable resistive strain sensors based on microstructured metal nanowire/elastomer composite films. *Small* **2018**, 14, 1704232. DOI: 10.1002/smll.201704232

19. Mo, F.; Huang, Y.; Li, Q.; Wang, Z.; Jiang, R.; Gai, W.; Zhi, C. A highly stable and durable capacitive strain sensor based on dynamically super-tough hydro/organo-gels. *Adv. Funct. Mater.* **2021**, 31, 2010830. DOI: 10.1002/adfm.202010830

20. Liang, H.; He, Y.; Chen, M.; Jiang, L.; Zhang, Z.; Heng, X.; Yang, L.; Hao, Y.; Wei, X.; Gan, J.; Yang, Z. Self-powered stretchable mechanoluminescent optical fiber strain sensor. *Adv. Intell. Syst.* **2021**, 3, 2100035. DOI: 10.1002/aisy.202100035

21. Gu, J.; Kwon, D.; Ahn, J.; Park, I. Wearable strain sensors using light transmittance change of carbon nanotube-embedded elastomers with microcracks. *ACS Appl. Mater. Interfaces* **2020**, 12, 10908-10917. DOI: 10.1021/acsami.9b18069

22. Butt, M. A.; Fomchenkov, S. A.; Ullah, A.; Verma, P.; Khonina, S. N. Biomedical bandpass filter for fluorescence microscopy imaging based on TiO_2/SiO_2 and TiO_2/MgF_2 dielectric multilayers. *J. Physics: Conf. Series* **2016**, 741, 012136. DOI 10.1088/1742-6596/741/1/012136

23. Kim, Joohoon, et al. Photonic encryption platform via dual-band vectorial metaholograms in the ultraviolet and visible. *ACS nano*, 2022, 16.3: 3546–3553

24. Ahn, J.; Ha, J. H.; Jeong, Y.; Jung, Y.; Choi, J.; Gu, J.; Hwang, S. H.; Kang, M.; Ko, J.; Cho, S.; Han, H.; Kang, K.; Park, J.; Jeon, S.; Jeong, J. H.; Park, I. (2023). Nanoscale three-dimensional fabrication based on mechanically guided assembly. *Nature Communications*, **2023**, 14, 833. DOI: 10.1038/s41467-023-36302-9

25. Zhao, Z. J.; Ahn, J.; Ko, J.; Jeong, Y.; Bok, M.; Hwang, S. H.; Kang, H. J.; Jeon, S.; Choi, J.; Park, I.; Jeong, J. H. Shape-controlled and well-arrayed heterogeneous nanostructures via

melting point modulation at the nanoscale. *ACS Appl. Mater. Interfaces* **2021**, 13, 3358–3368. DOI: 10.1021/acsami.0c18122

26. Ahn, J.; Kim, J. S.; Jeong, Y.; Hwang, S.; Yoo, H.; Jeong, Y.; Gu, J.; Mahato, M.; Ko, J.; Jeon, S.; Ha, J. H.; Seo, H. S.; Choi, J.; Kang, M.; Han, C.; Cho, Y.; Lee, C. H.; Jeong, J. H.; Oh, I. K.; Park, I. All-recyclable triboelectric nanogenerator for sustainable ocean monitoring systems. *Adv. Energy Mater.* **2022**, 12, 2201341. DOI: 10.1002/aenm.202201341

Table of Contents